Radiology

Well-aerated Lung on Admitting Chest CT to Predict Adverse Outcome in COVID-19 Pneumonia

Davide Colombi, MD • Flavio C. Bodini, MD • Marcello Petrini, MD • Gabriele Maffi, MD • Nicola Morelli, MD • Gianluca Milanese, MD • Mario Silva, MD, PhD • Nicola Sverzellati, MD, PhD • Emanuele Michieletti, MD

From the Department of Radiological Functions, Radiology Unit, Guglielmo da Saliceto Hospital, Via Taverna 49, 29121, Piacenza, Italy (D.C., F.C.B., M.P., G. Maffi, N.M., E.M.); and Department of Medicine and Surgery (DiMeC), University of Parma, Parma, Italy (G. Milanese, M.S., N.S.). Received April 6, 2020; revision requested April 8; revision received April 12; accepted April 14. **Address correspondence to** D.C. (e-mail: *D.Colombi@ausl.pc.it*).

Conflicts of interest are listed at the end of this article.

Radiology 2020; 296:E86–E96 • https://doi.org/10.1148/radiol.2020201433 • Content codes: CH CT

Background: CT of patients with severe acute respiratory syndrome coronavirus 2 disease depicts the extent of lung involvement in coronavirus disease 2019 (COVID-19) pneumonia.

Purpose: To determine the value of quantification of the well-aerated lung (WAL) obtained at admission chest CT to determine prognosis in patients with COVID-19 pneumonia.

Materials and Methods: Imaging of patients admitted at the emergency department between February 17 and March 10, 2020 who underwent chest CT were retrospectively analyzed. Patients with negative results of reverse-transcription polymerase chain reaction for severe acute respiratory syndrome coronavirus 2 at nasal-pharyngeal swabbing, negative chest CT findings, and incomplete clinical data were excluded. CT images were analyzed for quantification of WAL visually (%V-WAL), with open-source software (%S-WAL), and with absolute volume (VOL-WAL). Clinical parameters included patient characteristics, comorbidities, symptom type and duration, oxygen saturation, and laboratory values. Logistic regression was used to evaluate the relationship between clinical parameters and CT metrics versus patient outcome (intensive care unit [ICU] admission or death vs no ICU admission or death). The area under the receiver operating characteristic curve (AUC) was calculated to determine model performance.

Results: The study included 236 patients (59 of 123 [25%] were female; median age, 68 years). A %V-WAL less than 73% (odds ratio [OR], 5.4; 95% confidence interval [CI]: 2.7, 10.8; $P < .001$), %S-WAL less than 71% (OR, 3.8; 95% CI: 1.9, 7.5; $P < .001$), and VOL-WAL less than 2.9 L (OR, 2.6; 95% CI: 1.2, 5.8; $P < .01$) were predictors of ICU admission or death. In comparison with clinical models containing only clinical parameters (AUC = 0.83), all three quantitative models showed better diagnostic performance (AUC = 0.86 for all models). The models containing %V-WAL less than 73% and VOL-WAL less than 2.9 L were superior in terms of performance as compared with the models containing only clinical parameters ($P = .04$ for both models).

Conclusion: In patients with confirmed coronavirus disease 2019 pneumonia, visual or software quantification of the extent of CT lung abnormality were predictors of intensive care unit admission or death.

Online supplemental material is available for this article.

A novel coronavirus (severe acute respiratory syndrome coronavirus 2) has been considered the pathogen responsible for causing coronavirus disease 2019 (COVID-19), which has been spreading throughout the world since December 2019 (1). COVID-19 was declared a pandemic by the World Health Organization on March 11, 2020. Clinical expressions of COVID-19 range from flu-like symptoms to respiratory failure (ie, diffuse alveolar damage), the management of which demands advanced respiratory assistance and artificial ventilation.

Triage of patients with COVID-19 is based on clinical and laboratory parameters, whereas chest imaging might be required for second-level triage in specific cases, namely the chest radiography is offered as a first step and supplementary CT in more severe cases or in the case of discrepancies between clinical and radiographic characteristics (2,3). However, during the first phases of the COVID-19 outbreak, most unprepared facilities reported times for swab analysis of more than 24 hours, which significantly affected the management of emergency department patient flow. Some centers tried to manage this issue by switching from radiography to CT in a clinically integrated quick workflow (3). Li et al demonstrated that visual quantitative analysis of CT abnormalities reflects clinical categories of COVID-19 (4). Moreover, lung involvement of COVID-19 pneumonia could be assessed automatically with deep-learning–based quantitative CT (5).

However, the presence of coexisting chronic pulmonary abnormalities (eg, emphysema or interstitial lung diseases) was not accounted for in prior studies (4). Of note, CT quantification of well-aerated lung (WAL) was shown to be helpful either in the estimation of alveolar recruitment during ventilation or in the prediction of the prognosis of patients with acute respiratory distress syndrome (ARDS) (6,7).

The aim of this study was to describe the relationship between COVID-19 prognosis and the extent of

Abbreviations

ARDS = acute respiratory distress syndrome, CI = confidence interval, COVID-19 = coronavirus disease 2019, ICU = intensive care unit, OR = odds ratio, %S-WAL = software-based assessment of WAL percentage, %V-WAL = visual assessment of WAL percentage, VOL-WAL = software-based assessment of WAL absolute volume, WAL = well-aerated lung

Summary

Visual and software-based quantification of well-aerated lung parenchyma on admission chest CT scans were predictors of intensive care unit admission or death in patients with coronavirus disease 2019 pneumonia.

Key Results

- Patients with coronavirus disease 2019 pneumonia at baseline chest CT who were admitted to the intensive care unit (ICU) or who died had four or more lobes of the lung affected compared with patients who were not admitted to the ICU or who did not die (94% vs 84% of patients, $P < .04$).
- After adjustment for patient demographics and clinical parameters, visually assessed well-aerated lung parenchyma at admission on chest CT scans less than 73% was associated with ICU admission or death (odds ratio, 5.4; $P < .001$); software methods for lung quantification showed similar results.

WAL obtained with chest CT with either visual or quantitative measurements.

Materials and Methods

Study Population

This retrospective study was approved by the local ethics committee (Area Vasta Emiia-Nord) of our institution (Guglielmo da Saliceto Hospital) (institutional review board approval number, 241/2020/OSS/AUSLPC). The requirement for informed consent was waived because of the retrospective nature of the study. The study included consecutive patients suspected of having COVID-19 interstitial pneumonia who underwent chest CT upon emergency department admission between February 17 and March 10, 2020. All the patients underwent nasal-pharyngeal swabbing prior to a reverse-transcription polymerase chain reaction assay for severe acute respiratory syndrome coronavirus 2. A rapid (results in minutes to hours) COVID-19 reverse-transcription polymerase chain reaction test was not available at our center during this period. Thus, chest CT was performed on the basis of high clinical suspicion for COVID-19 and clinical and laboratory findings consistent with a diagnosis of COVID-19 in the setting of high pretest probability (ie, high community disease burden) (3,8).

To select chest CT scans for analysis, our exclusion criteria were reverse-transcription polymerase chain reaction for severe acute respiratory syndrome coronavirus 2 results that ultimately were negative, negative chest CT findings, incomplete clinical data, or a combination thereof. Figure 1 shows the patient enrollment flowchart.

Clinical and laboratory findings in each patient were recorded at admission. CT was performed within 12 hours after the clinical evaluation and laboratory findings.

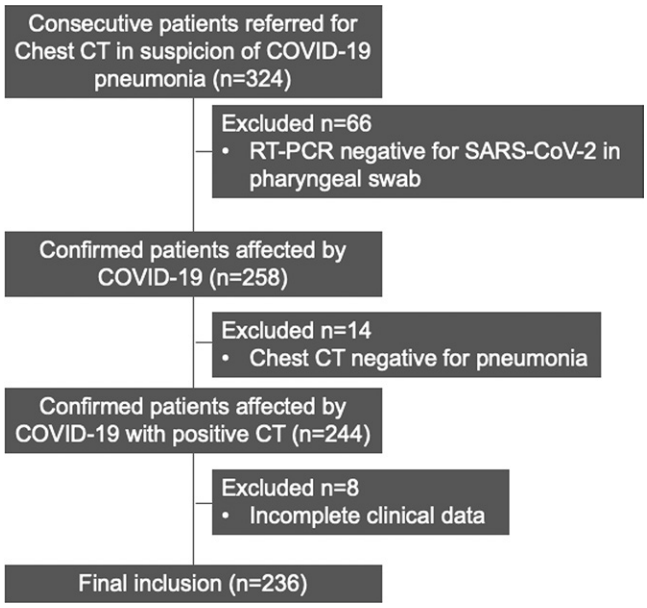

Figure 1: Diagram shows the patient selection process. COVID-19 = coronavirus disease 2019, RT-PCR = reverse-transcription polymerase chain reaction, SARS-CoV-2 = severe acute respiratory syndrome coronavirus 2.

Patients were categorized into two groups: *(a)* those who were admitted to the intensive care unit (ICU) or who died and *(b)* those who were discharged from the hospital alive without ICU admission. The time between CT and ICU admission or death was also registered.

CT Protocol

Unenhanced chest CT was performed in the supine position during an inspiratory breath hold, moving from the apex to the lung bases, with a 16-slice scanner (Emotion 16; Siemens, Forchheim, Germany). Low-dose CT acquisition was performed with the following parameters: tube voltage, 110 kV if body weight was 80 kg or less and 130 kV if patients weighed more than 80 kg; tube current, 40 mAs; pitch, one; and collimation, 0.625 mm. Image data sets were reconstructed with 1–2-mm slice thickness using both sharp kernels (B70f) with standard lung window settings (window width, 1500 HU; window center, −500 HU) and medium-soft kernels (B40f) with soft-tissue window settings (window width, 300 HU; window center, 40 HU).

CT Image Analysis

Visual scoring was performed independently by two radiologists (D.C., F.C.B.; 5 and 14 years of experience, respectively) who were blinded to clinical data. The total extent of WAL parenchyma expressed as a percentage of total lung volume was estimated to the nearest 5%. Scores derived from three lung zones (the upper zone, above the level of the carina; the lower zone, below the level of the infrapulmonary vein; and the middle zone, between the upper and lower zones) were averaged to yield a global percentage of WAL parenchyma (%V-WAL) (9,10). Consensus formulation for the visual scores was obtained as reported in the study by Cottin et al (11). The 5% most divergent observations for CT parameters and

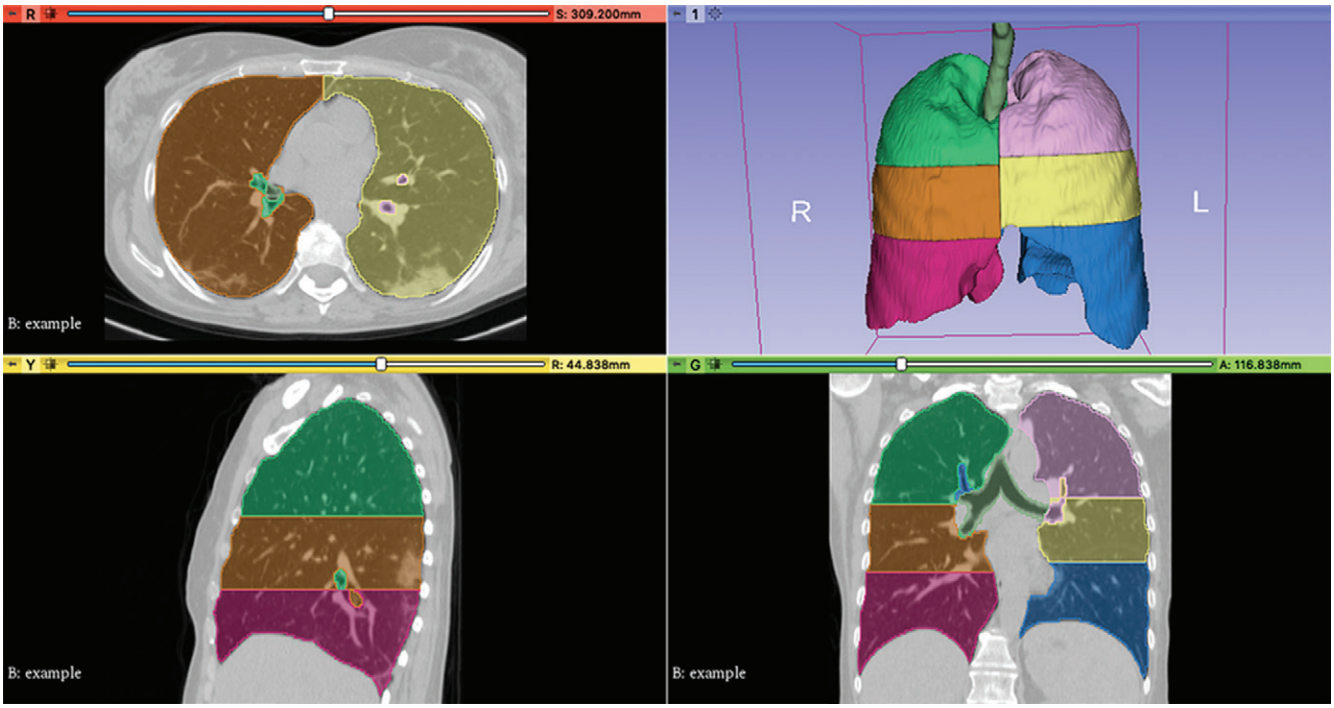

Figure 2: The Chest Imaging Platform extension (Applied Chest Imaging Laboratory; Boston, Mass) implemented in 3D Slicer software (version 4.10.2, *https://www.slicer.org*) was used to perform fully automatic segmentation of lung parenchyma. The algorithm yields a color map of the upper, middle, and lower zones of lung segmentation displayed with multiplanar reconstructions (axial, sagittal, and coronal) and in three-dimensional (3D) volume-rendered reconstruction. This example shows images in a 54-year-old woman with coronavirus disease 2019 pneumonia.

instances of discordance over the categorical CT assessment were resolved by consensus. The mean of the observer values was used for the remaining CT parameters (11). The patterns of CT abnormalities for diagnosis of COVID-19 were classified as defined in Table E1 (online): typical, indeterminate, or atypical (12). The number of involved lobes (zero to five) was registered. The prevalence in the upper, middle, or lower zone as defined earlier in this article was recorded. The axial distribution was classified as peripheral (prevalent in the outer third of the lung) or central (predominant in the inner two-thirds of the lung). The distribution pattern was classified as diffuse when a clear predominant craniocaudal or axial distribution was absent. Furthermore, the presence of mediastinal nodes enlargement (≥10 mm in short axis), pleural effusion, emphysema, and pulmonary fibrosis was assessed. The presence of breathing artifact was also recorded.

The software-based evaluation of the WAL parenchyma was performed at a dedicated workstation by using the extension Chest Imaging Platform (Applied Chest Imaging Laboratory, Boston, Mass) of the open-source 3D Slicer software, version 4.10.2 *(https://www.slicer.org)* (13). A fully automatic lung segmentation and analysis of lung parenchyma histogram was obtained by using B40f kernel (Fig 2). In case of unsatisfactory lung segmentation, the user amended the lung contours with a manual tool. The definition of normal lung by software segmentation (%S-WAL) was determined by density references from the literature, namely in the interval between −950 and −700 HU (14,15). Furthermore, using the overall lung volume provided by software, the absolute volume of the well-aerated lung (VOL-WAL) was calculated. The adipose tissue volume was calculated to assess obesity as a comorbidity and as a crude estimate of patient size (height and weight were not available). Adipose tissue volume was estimated by density interval between −170 and −40 HU on one slice at the T7–T8 level (16). The time to accomplish the software-based processing and the requirement of manual correction were recorded for each patient.

Statistical Analysis

Categorical variables are expressed as counts and percentages with corresponding 95% confidence intervals (CIs) using the Wilson method. Continuous variables are shown as medians and 95% CIs. The differences between the two groups were assessed with the Mann-Whitney *U* test for continuous variables and the χ^2 or Fisher exact test for categorical variables, as appropriate. The intraclass correlation coefficient was used to test interrater agreement for the %V-WAL and the concordance between %V-WAL and %S-WAL; the interpretation of the intraclass correlation coefficient was based on the guidelines provided by Koo and Li (17).

The outcome was defined by admission to the ICU or death. Categories from continuous variables were obtained and used as thresholds for the median value of the overall sample. For the CT metrics tested, additional categories were obtained using cutoffs derived from quartiles. Univariable and backward stepwise multivariable logistic regression analyses were used to test the association between potential predictors and outcome. Factors for which $P < .1$ in univariable analysis were used as candidate variables for the multivariable approach. Thus, a model

Table 1: Patient Characteristics, Comorbidities, Symptoms, and Laboratory Findings at Admission

Variable	All Patients (*n* = 236)	Patients without ICU Admission or Death (*n* = 128)	Patients with ICU Admission or Death (*n* = 108)	*P* Value
Age (y)	68 [66, 70]	62 [57, 66]	73 [71, 75]	<.001*
Sex				.88
Male	177 (75) [69, 80]	97 (76) [67, 82]	80 (74) [65, 81]	…
Female	59 (25) [19, 31]	31 (24) [17, 32]	28 (26) [18, 35]	…
Smoking history				.29
Unknown	156 (66) [60, 71]	84 (65) [57, 73]	72 (66) [57, 75]	…
Never	49 (21) [16, 26]	31 (25Z) [17, 32]	18 (17) [11, 25]	…
Current	6 (3) [1, 5]	3 (2) [0, 1]	3 (2) [1, 8]	…
Former	25 (10) [7, 15]	10 (8) [4, 14]	15 (15) [8, 21]	…
Comorbidity				
Cardiovascular	127 (54) [47, 60]	50 (39) [31, 48]	77 (71) [62, 78]	<.001*
Pulmonary	40 (17) [13, 23]	18 (14) [10, 21]	22 (20) [14, 29]	.27
Oncologic	35 (15) [11, 20]	10 (8) [4, 14]	25 (23) [16, 32]	<.01*
Neurologic	40 (17) [13, 22]	16 (12) [8, 19]	24 (22) [15, 31]	.07
Chronic kidney failure	15 (6) [4, 10]	3 (2) [1, 7]	12 (11) [6, 18]	.01*
Hepatic failure	5 (2) [1, 5]	2 (1) [0, 5]	3 (3) [1, 8]	.84
Diabetes	37 (16) [11, 21]	15 (11) [7, 18]	22 (20) [13, 28]	.1
Symptom				
Fever	230 (97) [94, 98]	123 (96) [91, 98]	107 (99) [94, 99]	.3
Cough	144 (61) [54, 67]	77 (60) [51, 68]	67 (62) [52, 70]	.87
Dyspnea	83 (35) [29, 41]	36 (28) [21, 36]	47 (43) [34, 52]	.02*
Asthenia	28 (12) [8, 16]	15 (12) [7, 18]	13 (12) [7, 19]	.89
Other	47 (20) [15, 25]	23 (18) [13, 25]	24 (22) [15, 31]	.51
Symptom onset (d)	5 (5, 7)	6 (5, 7)	5 (4, 7)	.06
Temperature at admission (°C)	37.7 (37.4, 37.9)	37.5 (37.1, 37.8)	37.8 (37.5, 38.3)	.1
SpO_2 (%)	93 (92, 94)	94 (93, 95)	91 (88, 92)	<.001*
White blood count ($\times 10^3/\mu L$)	5.6 (5.2, 6.2)	5.2 (4.7, 5.7)	6.8 (5.7, 7.6)	<.001*
Lymphocytes count ($\times 10^3/\mu L$)	1.02 (0.98, 1.1)	1.1 (1.02, 1.2)	0.87 (0.8, 1.01)	<.01*
Platelet count ($\times 10^3/\mu L$)	180 (164, 191)	160 (152, 170)	203 (186, 223)	<.001*
Lactate dehydrogenase (U/L)	347 (325, 376)	308 (281, 331)	435 (411, 465)	<.001*
CRP level (mg/dL)	7.6 (6.4, 8.6)	5.1 (4.1, 6)	13.3 (11.5, 14.1)	<.001*
eGFR level (mL/min/1.73 m^2)	76 (71, 81)	84 (78, 88)	69 (61, 73)	<.001*
GOT level (U/L)	41 (38, 44)	36 (33, 39)	46 (42, 54)	<.001*
GPT level (U/L)	30 (27, 33)	30 (25, 34)	31 (27, 37)	.9

Note.—Unless otherwise indicated, data are numbers of patients, and data in parentheses are percentages. Data in brackets are 95% confidence intervals (CIs) and were obtained by using the Wilson method. CRP = C-reactive protein, eGFR = estimated glomerular filtration rate, GOT = glutamic oxaloacetic transaminase, GPT = glutamic pyruvic transaminase, SpO_2 = peripheral oxygen saturation. To convert CRP to SI units (nanomoles per liter), multiply by 95.24. To convert lactate dehydrogenase to SI units (microkatals per liter), please multiply by 0.0167.

* $P < .05$ indicates a significant difference.

was obtained by using only clinical parameters; additional models were calculated by adding categories derived from quartiles of %V-WAL, %S-WAL, and VOL-WAL. The R^2 value of each model was then reported for comparison. Receiver operating characteristic curve analysis was performed for each model, and the area under the receiver operating characteristic curve (AUC) was used to assess the performance of the discrimination models based on independent predictors. The receiver operating characteristic curves of the two models were compared using the method of DeLong et al (18). $P < .05$ was considered indicative of a significant difference. Statistical analysis was performed using MedCalc software, version 14.8.1 (MedCalc Software, Ostend, Belgium).

Results

Patient Characteristics, Clinical, and Laboratory Findings

Patient characteristics and clinical and laboratory findings are reported in Table 1. The study included 236 patients (median age, 68 years; 95% CI: 66, 70), 59 of whom were female (25%; 95% CI: 19%, 31%). Cardiovascular diseases were the most frequent comorbidities (127 of 236; 54%; 95% CI: 47%, 60%), and admission laboratory findings showed elevated median lactate dehydrogenase (347 U/L; 95% CI: 325, 376) and C-reactive protein (7.6 mg/dL; 95% CI: 6.4, 8.6) values; furthermore, the median platelet count was 180 × $10^3/\mu L$ (95% CI: 164, 191). The ICU or death group included 108 of 236 patients (46%;

Table 2: CT Findings

CT Finding	Overall (*n* = 236)	Patients without ICU Admission or Death (*n* = 128)	Patients with ICU Admission or Death (*n* = 108)	*P* Value
Typical pattern				
Patchy GGO	63 (27) [21, 32]	43 (33) [26, 42]	20 (18) [12, 27]	.03*
Diffuse GGO	19 (8) [5, 12]	4 (3) [1, 8]	15 (14) [9, 22]	…
GGO and consolidation	119 (50) [44, 57]	69 (53) [45, 62]	50 (46) [37, 56]	…
Indeterminate pattern	29 (12) [8, 17]	10 (8) [4, 14]	19 (18) [11, 26]	…
Atypical pattern	6 (3) [1, 5]	2 (3) [1, 5]	4 (4) [1, 9]	…
Bilateral	223 (94) [91, 97]	123 (96) [91, 98]	100 (93) [86, 96]	.49
Craniocaudal distribution				
Diffuse	41 (18) [13, 23]	23 (18) [12, 25]	18 (17) [11, 25]	.27
Upper zone	58 (24) [19, 30]	26 (20) [14, 28]	32 (30) [22, 38]	…
Middle zone	34 (15) [10, 19]	17 (14) [8, 20]	17 (15) [11, 24]	…
Lower zone	103 (43) [37, 50]	62 (48) [40, 57]	41 (38) [29, 47]	…
Axial distribution				
Diffuse	174 (73) [68, 79]	83 (64) [56, 72]	91 (84) [76, 90]	<.001*
Central	5 (2) [1, 4]	1 (1) [0, 4]	4 (4) [1, 9]	…
Peripheral	57 (25) [19, 30]	44 (35) [27, 43]	13 (12) [7, 19]	…
Involved lobes				
≤3 lobes	27 (12) [8, 16]	20 (16) [10, 22]	7 (6) [3, 13]	.04*
>3 lobes	209 (88) [83, 92]	108 (84) [77, 89]	101 (94) [87, 96]	…
Pleural effusion	47 (20) [15, 25]	19 (15) [9, 22]	28 (26) [19, 35]	.06
Mediastinal nodes enlargement	57 (24) [19, 30]	24 (19) [13, 26]	33 (31) [23, 40]	.06
Emphysema	53 (22) [18, 28]	21 (16) [11, 24]	32 (29) [21, 38]	.02*
Pulmonary fibrosis	8 (3) [2, 7]	3 (2) [1, 7]	5 (5) [2, 10]	.54
Well-aerated lung, visual score (%)	73 (70, 77)	80 (77, 83)	53 (43, 57)	<.001*
Well-aerated lung, software-based score (%)	71 (68, 75)	78 (75, 80)	57 (52, 61)	<.001*
Well-aerated lung parenchyma (L)	2.9 (2.6, 3.1)	3.4 (3.1, 3.6)	2.3 (2, 2.5)	<.001*
Adipose tissue area at T7–T8 level (cm^2)	189 (177, 201)	170 (164, 180)	208 (194, 255)	<.001*

Note.—Unless otherwise indicated, data are numbers of patients, and data in parentheses are percentages. Data in brackets are 95% confidence intervals [CIs] and were calculated with the Wilson method. GGO = ground-glass opacity, ICU = intensive care unit.

* $P < .05$ indicates a significant difference.

95% CI: 40%, 52%). The median time elapsed between CT and the occurrence of ICU admission or death was 4 days (95% CI: 3, 6). Patients who were admitted to the ICU or who died were older (median age, 73 vs 62 years; $P < .001$) than those without ICU admission or death. In addition, the ICU or death group had a higher prevalence of cardiovascular diseases (71% vs 39%, $P < .001$), higher median lactate dehydrogenase levels (435 vs 308 U/L, $P < .001$), higher C-reactive protein levels (13.3 vs 5.1 mg/dL, $P < .001$), and higher platelet counts ([203 vs 160] × 10^3/μL, $P < .001$), respectively.

CT Findings

CT findings are summarized in Table 2. The majority (201 of 236; 85%; 95% CI: 80%, 89%) of the study subjects displayed a typical COVID-19 pneumonia CT pattern, whereas an indeterminate CT pattern was observed in 29 of 236 cases (12%; 95% CI: 8%, 17%). A variable combination of ground-glass opacities and consolidations were the main CT patterns (119 of 236; 50%; 95% CI: 44%, 57%). A lower zone predominance (103 of 236; 43%; 95% CI: 37%, 50%) and diffuse distribution in the axial plane (174 of 236; 73%; 95% CI: 68%, 79%) were the two most common distribution patterns. Concomitant emphysema was documented in 53 of 236 patients (22%; 95% CI: 18%, 28%), whereas pulmonary fibrosis was documented in eight of 236 patients (3%; 95% CI: 2%, 7%). Breathing artifacts were observed in 55 of 236 (23%; 95% CI: 18%, 29%) CT scans.

Patients with ICU admittance or death versus those with no ICU admittance or death had a higher number of lobes involved at CT (94% vs 84% with four or more lobes involved, $P = .04$) and had a higher prevalence of emphysema (29% vs 16%, $P = .02$), respectively.

The median %V-WAL was 73% (95% CI: 70%, 77%). Interrater agreement was good (intraclass correlation coefficient, 0.85; 95% CI: 0.77, 0.9).

Software analysis revealed a median %S-WAL of 71% (95% CI: 68%, 75%) and a median VOL-WAL of 2.9 L (95% CI: 2.6, 3.1). The distribution of visual and software-based CT parameters is shown in Figure 3. The median time required to achieve the software analysis was 270 seconds (95% CI: 240, 306), with a manual correction rate necessary in 143 of 236 cases (61%; 95% CI: 54%, 66%).

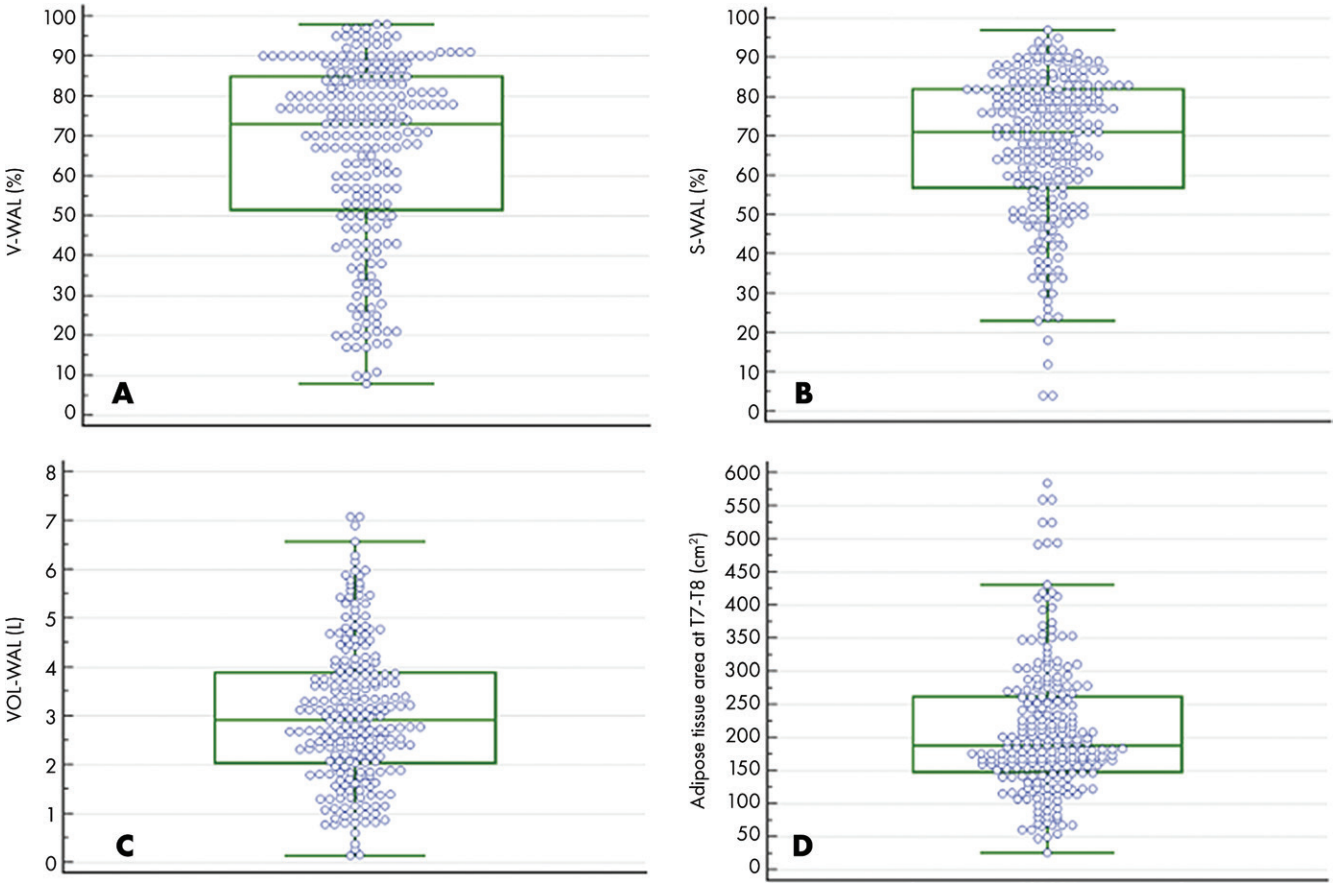

Figure 3: Box-and-whisker plots show the distribution of CT parameters. *A*, Median percentage of the well-aerated lung assessed visually (V-WAL) was 73% (interquartile range, 51%–85%). *B*, The median percentage of the well-aerated lung assessed with software (S-WAL) was 71% (interquartile range, 57%–82%). *C*, The absolute volume of the well-aerated lung (VOL-WAL) median value was 2.9 L (interquartile range, 2–3.9 L). *D*, The median value of the adipose tissue area at the level of T7–T8 was 189 cm^2 (interquartile range, 149–262 cm^2).

The agreement between %V-WAL and %S-WAL was good (intraclass correlation coefficient, 0.76; 95% CI: 0.69, 0.81). The WAL was lower in the ICU admittance or death group versus the no ICU admittance or death group by either visual assessment (median %V-WAL, 53% vs 80%; $P < .001$) or software-based analysis (median %S-WAL, 57% vs 78%, $P < .001$; median VOL-WAL, 2.3 vs 3.4 L, $P < .001$).

The median adipose tissue area at the T7–T8 level was 189 cm^2 (95% CI: 177, 201). The median adipose tissue area at the T7–T8 level was higher in the ICU or death group versus the no ICU or death group (208 vs 170 cm^2, $P = .001$).

Logistic Regression Analysis

Table 3 and Tables E2–E4 (online) summarize uni- and multivariable logistic regression analysis results. In multivariable analysis performed with only clinical parameters (clinical model), the best predictors of ICU admittance or death were cardiovascular comorbidities (OR, 3.7; 95% CI: 1.9, 7.3; $P < .001$) and age of more than 68 years (OR, 3.4; 95% CI: 1.7, 6.6; $P < .001$).

For the CT metrics of WAL, we observed worse outcome with lower values of WAL parenchyma, which appears significant at the median values of WAL for both visual and software-based assessments (Tables E2–E4 [online]). Median values were used in subsequent assessments.

When CT visual assessment of WAL was added to the model with clinical parameters, a %V-WAL less than 73% (OR, 5.4; 95% CI: 2.7, 10.8; $P < .001$) was associated with ICU admittance or death (Table 4). Similar findings were confirmed with multivariable analysis results obtained with the software-based estimation of WAL (Figs 4, 5). For the software analysis, both %S-WAL less than 71% (OR, 3.8; 95% CI: 1.9, 7.5; $P < .001$) and VOL-WAL less than 2.9 L (OR, 2.6; 95% CI: 1.3, 5.2; $P < .01$) were independent predictors of ICU admittance or death.

An adipose tissue area at the T7–T8 level of more than 262 cm^2 was a predictor of the outcome in the two models with software-based assessment of CT (in the %S-WAL <71% model: OR, 3; 95% CI: 1.4, 6.5; in the VOL-WAL <2.9 L model: OR, 2.6, 95% CI: 1.2, 5.8; $P < .01$).

Diagnostic performance of the models is reported in Figure 6 and Table 4. The AUC for the clinical model was 0.83 (95% CI: 0.78, 0.88) with an R^2 of 0.31. The models that included clinical parameters and additional CT evaluation with both visual and software-based assessments showed higher AUC and R^2 as compared with the clinical model (eg, %V-WAL <73%: AUC = 0.86; 95% CI: 0.81, 0.9; $R^2 = 0.36$) with the same AUC values for both

Table 3: Logistic Regression Analysis for the Relationship between Baseline Clinical and CT Parameters to Predict ICU Admission or Death

							Multivariable Clinical and CT								
							Visual Assessment			Software-based Assessment					
	Univariable Analysis			Multivariable Clinical			%V-WAL < 73%			%S-WAL < 71%			VOL-WAL < 2.9 L		
Variable	Co	OR	*P* value	Co	OR	*P* value	Co	OR	*P* value	Co	OR	*P* value	Co	OR	*P* value
Age > 68 years	1.3	3.8 (2.2, 6.6)	<.001	1.2	3.4 (1.7, 6.6)	<.001	1.1	3.1 (1.5, 6.2)	<.01	1.1	3 (1.5, 6.0)	<.01	1.1	3.1 (1.5, 6.4)	<.01
CV comorbidities	1.3	3.8 (2.2, 6.7)	<.001	1.3	3.7 (1.9, 7.3)	<.001	1.4	4.2 (2.1, 8.5)	<.001	1.2	3.4 (1.7, 7.0)	<.001	1.2	3.5 (1.7, 7.1)	<.001
Oncological comorbidities	1.2	3.5 (1.6, 7.7)	<.01	…	…	…	…	…	…	…	…	…	…	…	…
Chronic kidney failure	1.6	5.2 (1.4, 18.9)	.01	…	…	…	…	…	…	…	…	…	…	…	…
Dyspnea	0.7	1.9 (1.1, 3.3)	.01	…	…	…	…	…	…	…	…	…	…	…	…
SpO_2 < 93%	1.3	3.6 (2.1, 6.2)	<.001	…	…	NS	…	…	NS	…	…	NS	…	…	NS
WBC > 5.6 × 10^3/μL	0.7	2.1 (1.2, 3.5)	<.01	…	…	…	…	…	…	…	…	…	…	…	…
Lymph < 1.02 × 10^3/μL	0.8	2.3 (1.3, 3.8)	<.01	…	…	…	…	…	…	…	…	…	…	…	…
PLT > 180 × 10^3/μL	1	2.8 (1.7, 4.8)	<.001	1	2.9 (1.4, 5.7)	<.01	1.1	3.2 (1.6, 6.5)	<.01	0.9	2.4 (1.1, 4.8)	.01	0.8	2.2 (1.1, 4.5)	.02
LDH > 347 U/L	1.4	4(2.3, 6.8)	<.001	1.1	3 (1.5, 5.9)	<.001	…	…	NS	…	…	NS	0.8	2.3 (1.1, 4.6)	.02
CRP > 7.6 mg/dL	1.6	4.9 (2.8, 8.4)	<.001	1	2.8 (1.5, 5.3)	<.01	0.7	2.1 (1.1, 4.2)	.03	0.8	2.3 (1.1, 4.5)	.02	0.8	2.2 (1.1, 4.4)	.02
eGFR < 76 mL/min/1.73 m^2	1.1	2.9 (1.7, 4.9)	<.001	…	…	NS	…	…	NS	…	…	NS	…	…	NS
GOT > 41 U/L	0.9	2.6 (1.5, 4.4)	<.001	…	…	…	…	…	…	…	…	…	…	…	…
Emphysema	0.8	2.1 (1.1, 4.0)	.02	…	…	…	…	…	…	…	…	…	…	…	…
%V-WAL < 85%	1.4	4 (2.7, 8.0)	<.001	…	…	…	…	…	…	…	…	…	…	…	…
%V-WAL < 73%	2	7.1 (4.0, 12.7)	<.001	…	…	…	1.7	5.4 (2.7, 10.8)	<.001	…	…	…	…	…	…
%V-WAL < 51%	2.8	16 (6.8, 37.5)	<.001	…	…	…	…	…	…	…	…	…	…	…	…
%S-WAL < 82%	1.1	3 (1.6, 5.6)	<.001	…	…	…	…	…	…	…	…	…	…	…	…
%S-WAL < 71%	1.7	5.6 (3.2, 9.9)	<.001	…	…	…	…	…	…	1.3	3.8 (1.9, 7.5)	<.001	…	…	…
%S-WAL < 57%	2.9	18.1 (7.3, 44.8)	<.001	…	…	…	…	…	…	…	…	…	…	…	…
VOL-WAL < 3.9 L	1.3	3.5 (1.8, 7.0)	<.001	…	…	…	…	…	…	…	…	…	…	…	…
VOL-WAL < 2.9 L	1.5	4.5 (2.6, 7.9)	<.001	…	…	…	…	…	…	…	…	…	0.9	2.6 (1.3, 5.2)	.01
VOL-WAL < 2 L	1.7	5.3 (2.7, 10.5)	<.001	…	…	…	…	…	…	…	…	…	…	…	…
AT > 149 cm^2	0.6	1.9 (1.0, 3.5)	.03	…	…	…	…	…	…	…	…	…	…	…	…

Table 3 *(continues)*

Table 3 *(continued)*: Logistic Regression Analysis for the Relationship between Baseline Clinical and CT Parameters to Predict ICU Admission or Death

							Multivariable Clinical and CT							
							Visual Assessment			Software-based Assessment				
	Univariable Analysis			Multivariable Clinical			%V-WAL < 73%			%S-WAL < 71%			VOL-WAL < 2.9 L	
Variable	Co	OR	*P* value	Co	OR	*P* value	Co	OR	*P* value	Co	OR	*P* value	Co	OR	*P* value
AT > 189 cm²	1	2.8 (1.6, 4.8)	<.001	…	…	…	…	…	…	…	…	…	…	…	…
AT > 262 cm²	1.5	4.6 (2.4, 8.8)	<.001	…	…	…	…	…	…	1.1	3.0 (1.4, 6.5)	<.01	1	2.6 (1.2, 5.8)	.01

Note.—Data in parentheses are 95% confidence intervals. Variables retained in the models are associated with ICU admission or death at the $P < .05$ level. AT = adipose tissue area measured at T7–T8 level, CI = confidence interval, Co = coefficient, CRP = C-reactive protein, CV = cardiovascular, eGFR = estimated glomerular filtrate rate, GOT = glutamic oxaloacetic transaminase, LDH = lactate dehydrogenase, lymph = lymphocytes, NS = nonsignificant, OR = odds ratio, PLT = platelet, SpO_2 = peripheral oxygen saturation, %S-WAL = well-aerated lung parenchyma percentage assessed by software, %V-WAL = well-aerated lung parenchyma percentage assessed visually, VOL-WAL = well-aerated lung parenchyma absolute volume assessed by software, WBC = white blood cell.

Table 4: Sensitivity, Specificity, PPV, NPV, AUC, and R^2 Values Derived from Logistic Regression Models for the Relationship between Baseline Clinical and CT Parameters to Predict ICU Admission or Death

Model	Sensitivity (%)	Specificity (%)	PPV (%)	NPV (%)	AUC	R^2 Value	*P* Value
Clinical model	75 (66, 82)	73 (65, 81)	70 (61, 78)	78 (72, 83)	0.83 (0.78, 0.88)	0.31	Reference
Model with clinical parameters and %V-WAL <73%	72 (63, 80)	81 (73, 88)	76 (68, 82)	78 (73, 83)	0.86 (0.81, 0.90)	0.36	0.04*
Model with clinical parameters, %S-WAL <71% and AT area >262 cm²	75 (66, 83)	80 (72, 86)	75 (68, 81)	80 (73, 85)	0.86 (0.80, 0.90)	0.36	0.06
Model with clinical parameters, VOL-WAL <2.9 L and AT area >262 cm²	75 (66, 83)	81 (73, 88)	77 (69, 83)	79 (74, 84)	0.86 (0.81, 0.90)	0.36	0.04*

Note.—Data in parentheses are 95% confidence intervals. The receiver operating characteristic (ROC) curves of the models were compared with the DeLong et al method (18). *P* values refer to the comparison between models including CT metrics and models including only clinical parameters. AT = adipose tissue area measured at T7–T8 level, AUC = area under the ROC curve, CI = confidence interval, ICU = intensive care unit, NPV = negative predictive value, PPV = positive predictive value, %S-WAL = well-aerated lung parenchyma percentage assessed by software, %V-WAL = well-aerated lung parenchyma percentage assessed visually, VOL-WAL = well-aerated lung parenchyma absolute volume assessed by software.

*$P < .05$ indicates a significant difference.

software approaches (AUC = 0.86). The models containing %V-WAL less than 73% or VOL-WAL less than 2.9 L were superior in terms of performance as compared with the models containing only clinical parameters ($P = .04$ for both models).

Discussion

Coronavirus disease 2019 (COVID-19) is associated with a variable prognosis. COVID-19 pneumonia requires mechanical ventilation in up to 17% of patients and shows mortality ranging from 11% to 15% (19,20). The results of the present study show that the proportion of well-aerated lung (WAL) assessed with chest CT obtained at admission in the emergency department was associated with better prognosis in patients with COVID-19 pneumonia independent of other clinical parameters. For example, patients with visually assessed WAL parenchyma less than 73% had a 5.4 (95% CI: 2.7, 10.8) times greater likelihood of intensive care unit admission or death, even after adjustment for clinical and demographic parameters. Similar overall prognostic performance of WAL parenchyma was observed for both visual scoring and computer analysis of WAL, supporting the robustness of the results. Although visual assessment of WAL had good interobserver agreement (intraclass correlation coefficient, 0.85) in a research setting, automated software measurement of WAL parenchyma could, in theory, offer greater reliability in the clinic (21).

A model used to predict mortality in patients with viral pneumonia (known as the MuLBSTA [multilobar infiltration, hypolymphocytosis, bacterial coinfection, smoking history, hypertension, age] score) including multilobar infiltrate at imaging also enabled prediction of death in patients with COVID-19 (19,22). Several methods to quantify disease extent with chest CT have been proposed, including measuring the extent of emphysema,

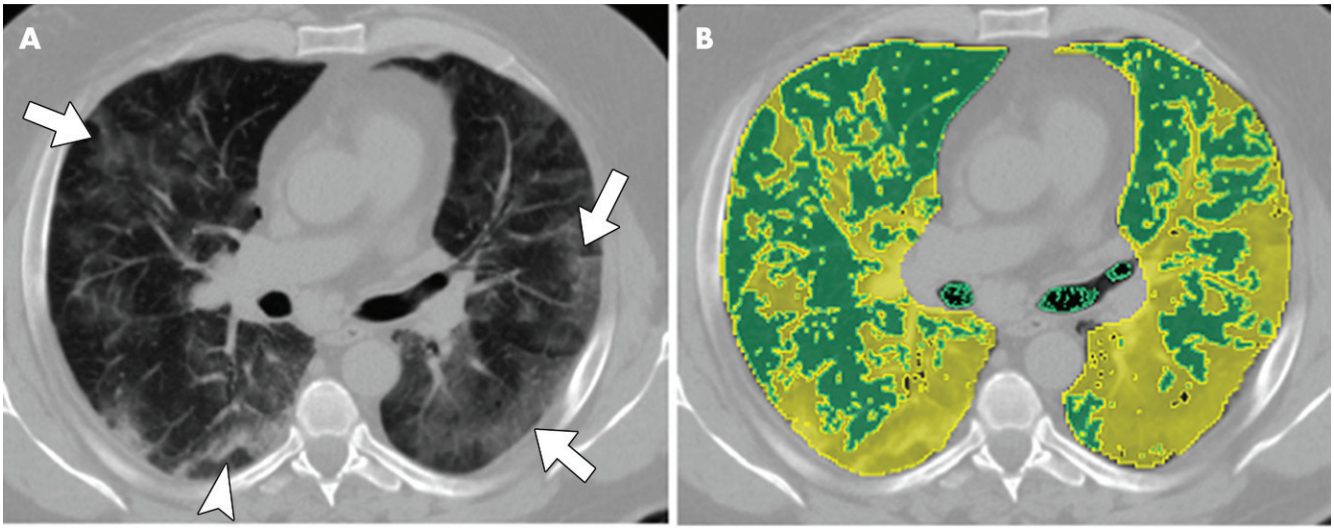

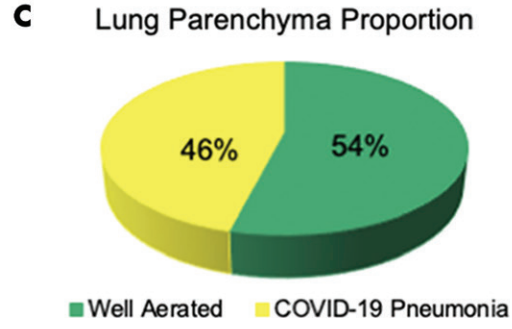

Figure 4: Images in a 65-year-old man with coronavirus disease 2019 (COVID-19) pneumonia admitted to intensive care unit. *A*, Unenhanced axial chest CT image shows bilateral patchy ground-glass opacities (arrows) with random distribution and peripheral bandlike consolidation in the right lower lobe (arrowhead), with visual quantification of the well-aerated lung of 35%. *B*, The same image as in, *A*, highlights the well-aerated lung (green) and COVID-19 pneumonia (yellow); the analysis of the relative density histogram, quantified as an overall well-aerated volume of 54%, corresponds to an absolute volume of 2.3 L. *C*, The three-dimensional pie chart shows the proportion of COVID-19 pneumonia and well-aerated lung parenchyma.

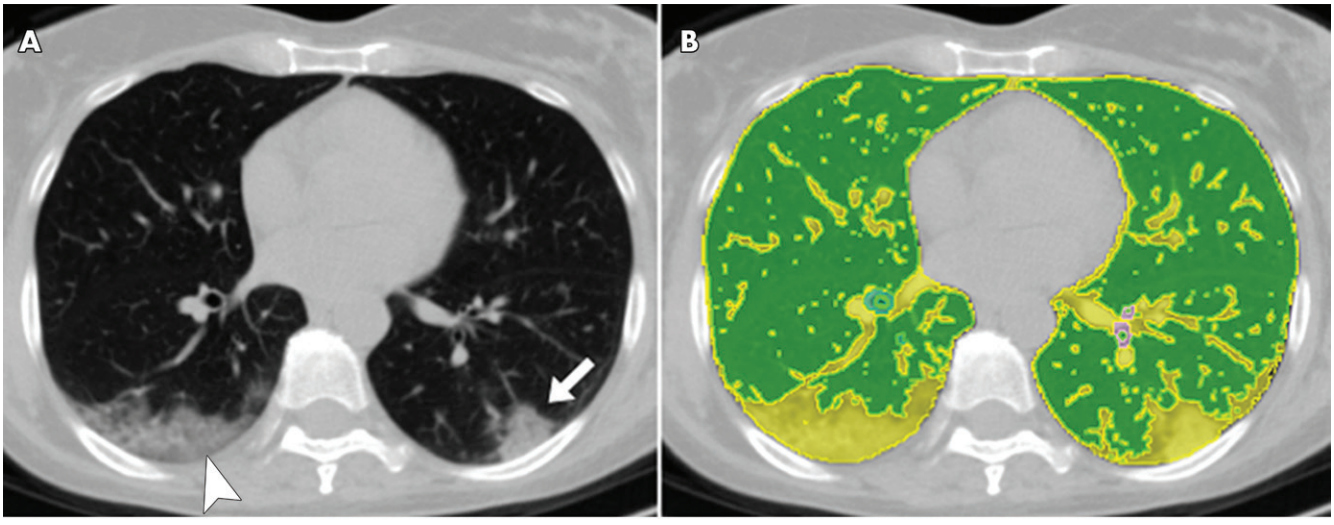

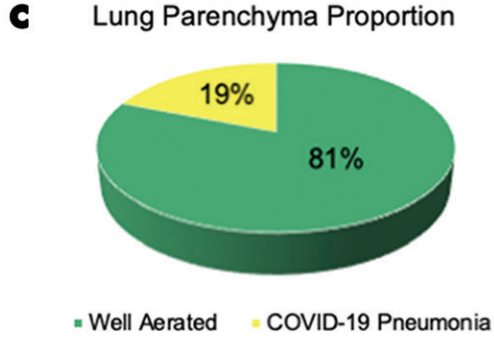

Figure 5: Images in a 54-year-old woman affected by coronavirus disease 2019 (COVID-19) pneumonia who was discharged home from the emergency department. *A*, Unenhanced axial chest CT image shows peripheral consolidation (arrow) in the left lower lobe and peripheral mixed crazy-paving opacities and consolidation in the right lower lobe (arrowhead), with visual quantification of the well-aerated lung of 85%. *B*, The same image as in, *A*, highlights the well-aerated lung (green) and COVID-19 pneumonia (yellow); the analysis of the relative density histogram, quantified as an overall well-aerated volume of 81%, corresponds to an absolute volume of 3.3 L. *C*, The three-dimensional pie chart shows the proportion of COVID-19 pneumonia and well-aerated lung parenchyma.

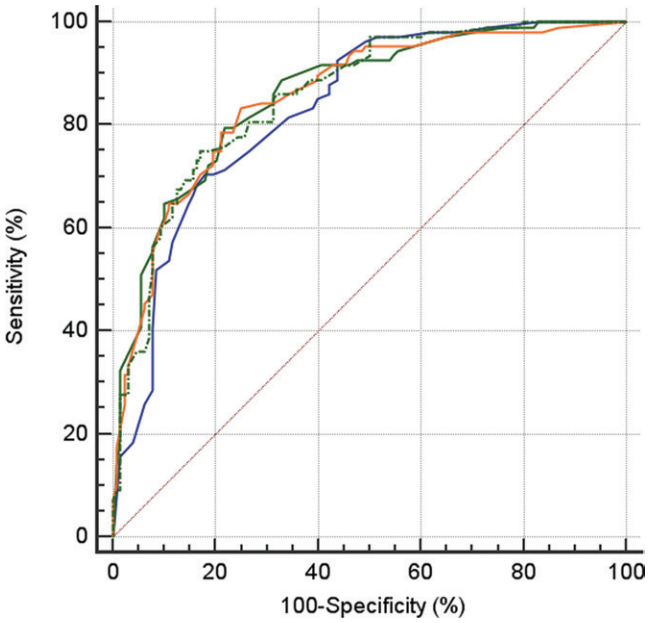

Figure 6: Graph shows diagnostic performance predicting intensive care unit admission or death for patients with coronavirus disease 2019 (COVID-19) based on baseline parameters and chest CT at emergency department admission. Receiver operator characteristic (ROC) curves of the models based on clinical parameters (blue line), clinical parameters and percentage of well-aerated lung as assessed visually (green solid line), by software histogram analysis (orange line) and as absolute volume (green dotted line). The area under the ROC curve (AUC) for the clinical model was 0.83 (95% confidence interval [CI]: 0.78, 0.88). The models including clinical parameters and additional CT evaluation of the well-aerated lung parenchyma assessed visually and with software showed higher performance as compared with the clinical model (%V-WAL <73%: AUC = 0.86; 95% CI: 0.81, 0.90; %S-WAL <71%: AUC = 0.86; 95% CI: 0.80, 0.90) (VOL-WAL: AUC = 0.86; 95% CI: 0.81, 0.90). %S-WAL = percentage of well-aerated lung assessed with software, %V-WAL = percentage of well-aerated lung assessed visually, VOL-WAL = absolute volume of well-aerated lung.

pulmonary fibrosis, and ARDS (8,13,23–25). CT score of the burden of lung disease was previously reported as a risk factor for mortality in patients with ARDS (8). However, there is scarce data on the prognostic value of CT in patients with COVID-19. A visual semiquantitative quantification of disease extent at CT correlated with clinical severity (26). However, underlying lung abnormalities (eg, emphysema or lung fibrosis) were not included in prior estimates of lung disease burden.

Well-ventilated regions of the lung may be a surrogate of residual respiratory function (6). Furthermore, the aerated lung in patients with ARDS is substantially reduced in volume and might represent an important parameter for the appropriate setting of mechanical ventilation main parameters, such as tidal volume (V_t) and positive end-expiratory pressure (27). To prevent ventilation-induced lung injury, the ratio of V_t to aerated lung (termed *baby lung*) should be applied rather than the ratio of V_t to patient weight (in kilograms) because it allows for maintenance of stress and strain within physiologic limits, as reported by Gattinoni and Pesenti (27). This parameter can be calculated only by software. In ARDS, a ratio of less than 40% between the WAL region noted at CT and the predicted total lung capacity was associated with a higher risk of death (6).

In consideration of the substantial rate of ARDS in patients with COVID-19 (17%), we hypothesized that the volume of WAL at admission CT may enable stratification of the disease severity. We tested patients at admission to the emergency department to predict ICU admission or death. Notably, ARDS criteria were not fulfilled at admission CT. Furthermore, our proposed cutoff of 70%–75% WAL parenchyma is considerably higher than the 40% cutoff reported in the literature to assess prognosis in patients with ARDS (6). We used density threshold differently than what has been suggested previously for ARDS, namely a range form of −900 HU indicating nearly 90% gas and 10% tissue to −500 HU indicating 50% gas and 50% tissue (28). Again, our −950 to −700 HU range is intended for patients with respiratory function at self-referral, and indeed, our definition reflects lung approximately completely ventilated as compared with severely compromised aerated lung in ARDS (14).

Our results also showed an association between adipose tissue area and worse outcome. Body mass index was not routinely recorded in our emergency department. However, obesity has been described as a common comorbidity in patients hospitalized for H1N1 influenza infection (29). Previous observations suggest COVID-19 will likely have a more severe course in obese patients (30). For this reason, CT evaluation of adipose tissue could be an objective hallmark of obesity with prognostic importance.

This study had several limitations. First, it was a retrospective analysis from one institution. Second, spirometric gating was not used in the acquisition of chest CT images because of the emergency setting. Best et al previously suggested that spirometric standardization might not be necessary for routine CT volume assessment (31). Third, the interrater agreement for software-based quantification was not calculated but is expected to be high as demonstrated in severe interstitial lung disease (32). Fourth, body size was not calculated.

In conclusion, both visual and software-based quantification of the well-aerated lung at chest CT in the emergency setting were independent predictors of intensive care unit admission or death in patients with coronavirus disease 2019 (COVID-19). Quantitative assessment of the extent of lung involvement by COVID-19 pneumonia may be useful for routine patient care.

Author contributions: Guarantors of integrity of entire study, D.C., F.C.B., N.M.; study concepts/study design or data acquisition or data analysis/interpretation, all authors; manuscript drafting or manuscript revision for important intellectual content, all authors; approval of final version of submitted manuscript, all authors; agrees to ensure any questions related to the work are appropriately resolved, all authors; literature research, D.C., F.C.B., M.P., G. Maffi, G. Milanese, M.S., N.S., E.M.; clinical studies, D.C., F.C.B., M.P., G. Maffi, N.M.; statistical analysis, D.C., M.P., M.S., E.M.; and manuscript editing, D.C., F.C.B., M.P., G. Maffi, G. Milanese, M.S., N.S., E.M.

Disclosures of Conflicts of Interest: D.C. disclosed no relevant relationships. **F.C.B.** disclosed no relevant relationships. **M.P.** disclosed no relevant relationships. **G. Maffi** disclosed no relevant relationships. **N.M.** disclosed no relevant relationships. **G. Milanese** disclosed no relevant relationships. **M.S.** disclosed no relevant relationships. **N.S.** Activities related to the present article: disclosed no relevant relationships. Activities not related to the present article: is a consultant for Galapagos and Boehringer Ingelheim; institution received grants from Roche, Boehringer Ingelheim, and Chiesi; gave lectures for Roche, Boehringer Ingelheim, and Chiesi. Other relationships: disclosed no relevant relationships. **E.M.** disclosed no relevant relationships.

References

1. Li Q, Guan X, Wu P, et al. Early Transmission Dynamics in Wuhan, China, of Novel Coronavirus-Infected Pneumonia. N Engl J Med 2020;382(13):1199–1207.
2. American College of Radiology (ACR). ACR Recommendations for the use of chest radiography and computed tomography (CT) for suspected COVID-19 Infection. https://www.acr.org/Advocacy-and-Economics/ACR-Position-Statements/Recommendations-for-Chest-Radiography-and-CT-for-Suspected-COVID19-Infection. Published March 11, 2020. Accessed April 1, 2020.
3. Sverzellati N, Milanese G, Milone F, Balbi M, Ledda RE, Silva M. Integrated radiologic algorithm for COVID-19 pandemic. J Thorac Imaging Published online April 7, 2020. Accessed April 8, 2020..
4. Li K, Fang Y, Li W, et al. CT image visual quantitative evaluation and clinical classification of coronavirus disease (COVID-19). Eur Radiol Published online March 25, 2020. Accessed March 28, 2020..
5. Huang L, Han R, Ai T, et al. Serial quantitative chest CT assessment of COVID-19: deep-learning approach. Radiol Cardiothorac Imaging 2020; 2(2):e200075.
6. Nishiyama A, Kawata N, Yokota H, et al. A predictive factor for patients with acute respiratory distress syndrome: CT lung volumetry of the well-aerated region as an automated method. Eur J Radiol 2020;122:108748.
7. Gattinoni L, Caironi P, Cressoni M, et al. Lung recruitment in patients with the acute respiratory distress syndrome. N Engl J Med 2006;354(17):1775–1786.
8. Rubin GD, Ryerson CJ, Haramati LB, et al. The role of chest imaging in patient management during the COVID-19 pandemic: a multinational consensus statement from the Fleischner Society. Radiology Published online April 7, 2020. Accessed April 8, 2020.
9. Ichikado K, Muranaka H, Gushima Y, et al. Fibroproliferative changes on high-resolution CT in the acute respiratory distress syndrome predict mortality and ventilator dependency: a prospective observational cohort study. BMJ Open 2012;2(2):e000545.
10. Edey AJ, Devaraj AA, Barker RP, Nicholson AG, Wells AU, Hansell DM. Fibrotic idiopathic interstitial pneumonias: HRCT findings that predict mortality. Eur Radiol 2011;21(8):1586–1593.
11. Cottin V, Hansell DM, Sverzellati N, et al. Effect of emphysema extent on serial lung function in patients with idiopathic pulmonary fibrosis. Am J Respir Crit Care Med 2017;196(9):1162–1171.
12. Simpson S, Kay FU, Abbara S, et al. Radiological Society of North America Expert Consensus Statement on reporting chest CT findings related to COVID-19. Endorsed by the Society of Thoracic Radiology, the American College of Radiology, and RSNA. Radiol Cardiothorac Imaging 2020;2(2):e200152.
13. Fedorov A, Beichel R, Kalpathy-Cramer J, et al. 3D Slicer as an image computing platform for the Quantitative Imaging Network. Magn Reson Imaging 2012;30(9):1323–1341.
14. Chen A, Karwoski RA, Gierada DS, Bartholmai BJ, Koo CW. Quantitative CT analysis of diffuse lung disease. RadioGraphics 2020;40(1):28–43.
15. Matsuoka S, Yamashiro T, Matsushita S, et al. Quantitative CT evaluation in patients with combined pulmonary fibrosis and emphysema: correlation with pulmonary function. Acad Radiol 2015;22(5):626–631.
16. Tong Y, Udupa JK, Torigian DA, et al. Chest fat quantification via CT based on standardized anatomy space in adult lung transplant candidates. PLoS One 2017;12(1):e0168932.
17. Koo TK, Li MY. A guideline of selecting and reporting intraclass correlation coefficients for reliability research. [Published correction appears in J Chiropr Med 2017;16(4):346.] J Chiropr Med 2016;15(2):155–163.
18. DeLong ER, DeLong DM, Clarke-Pearson DL. Comparing the areas under two or more correlated receiver operating characteristic curves: a nonparametric approach. Biometrics 1988;44(3):837–845.
19. Chen N, Zhou M, Dong X, et al. Epidemiological and clinical characteristics of 99 cases of 2019 novel coronavirus pneumonia in Wuhan, China: a descriptive study. Lancet 2020;395(10223):507–513.
20. Huang C, Wang Y, Li X, et al. Clinical features of patients infected with 2019 novel coronavirus in Wuhan, China. [Published correction appears in Lancet 2020;395(10223):496.] Lancet 2020;395(10223):497–506.
21. Yoon RG, Seo JB, Kim N, et al. Quantitative assessment of change in regional disease patterns on serial HRCT of fibrotic interstitial pneumonia with texture-based automated quantification system. Eur Radiol 2013;23(3):692–701.
22. Guo L, Wei D, Zhang X, et al. Clinical features predicting mortality risk in patients with viral pneumonia: the MuLBSTA Score. Front Microbiol 2019;10:2752.
23. Sverzellati N, Odone A, Silva M, et al. Structured reporting for fibrosing lung disease: a model shared by radiologist and pulmonologist. Radiol Med (Torino) 2018;123(4):245–253.
24. Mohamed Hoesein FA, de Hoop B, Zanen P, et al. CT-quantified emphysema in male heavy smokers: association with lung function decline. Thorax 2011;66(9):782–787.
25. Maldonado F, Moua T, Rajagopalan S, et al. Automated quantification of radiological patterns predicts survival in idiopathic pulmonary fibrosis. Eur Respir J 2014;43(1):204–212.
26. Yang R, Li X, Liu H, et al. Severity Score: an imaging tool for assessing severe COVID-19. Radiol Cardiothorac Imaging 2020;2(2):e200047.
27. Gattinoni L, Pesenti A. The concept of "baby lung". Intensive Care Med 2005;31(6):776–784.
28. Gattinoni L, Pesenti A, Avalli L, Rossi F, Bombino M. Pressure-volume curve of total respiratory system in acute respiratory failure. Computed tomographic scan study. Am Rev Respir Dis 1987;136(3):730–736.
29. Venkata C, Sampathkumar P, Afessa B. Hospitalized patients with 2009 H1N1 influenza infection: the Mayo Clinic experience. Mayo Clin Proc 2010;85(9):798–805.
30. Dietz W, Santos-Burgoa C. Obesity and its Implications for COVID-19 Mortality. Obesity 2020;28(6):1005.
31. Best AC, Meng J, Lynch AM, et al. Idiopathic pulmonary fibrosis: physiologic tests, quantitative CT indexes, and CT visual scores as predictors of mortality. Radiology 2008;246(3):935–940.
32. Wang J, Li F, Li Q. Automated segmentation of lungs with severe interstitial lung disease in CT. Med Phys 2009;36(10):4592–4599.